Journal of Machine Engineering, 2025, Vol. 25
ISSN 1895-7595 (Print) ISSN 2391-8071 (Online)

Received*: 07 February 2025* / Accepted: *31 May 2025* / Published online: *25 August 2025*

condition monitoring,
linear guideways, load measurement,
inductive proximity sensor

Yutao LAN[1*], Danny STAROSZYK[1],
Mukesh MOGA[1], Jens MÜLLER[1],
Steffen IHLENFELDT[2,1]

REAL-TIME LOAD MONITORING IN LINEAR GUIDEWAYS USING INTEGRATED INDUCTIVE PROXIMITY SENSORS

Linear guideways are essential components of manufacturing technology, providing precise motion and supporting significant loads in machine tools and automated systems. Real-time load measurement in these guideways is critical for effective condition monitoring and predictive maintenance. However, the compact and integrated nature of linear guideway systems makes such measurements inherently challenging. This study presents a novel approach to measuring load using relatively inexpensive inductive proximity sensors integrated into the linear guideway. The proposed method estimates the load by analyzing the relative position between the rolling element and the carriage, which is determined using switching signals. The principle of the measurement method was validated in a preliminary study using a 3-axis machine tool and subsequently tested on a fatigue life test rig under various load conditions. The results are promising and demonstrate the potential of this method for real-time load monitoring.

1. INTRODUCTION

Linear guideways (LGW) are essential components in modern manufacturing engineering, playing an important role in machine tools and automated systems. They provide precise motion and support significant loads, which is vital for achieving high accuracy and reliability in industrial processes. As manufacturing systems evolve, there is an increasing demand for enhanced performance, minimal downtime, and extended equipment lifespan. In this context, condition monitoring and predictive maintenance have become key strategies, enabling proactive detection and resolution of potential failures [1].

When a load is applied to an LGW, both the rolling elements (RE) and the carriage undergo deformation [2]. Accurate service life prediction of LGWs requires precise determination of these loads during operation [3]. To improve prediction accuracy, sophisticated calculation models have been proposed e.g. [4, 5], in which the load is a critical

[1] Faculty of Mechanical Engineering, Institute of Mechatronic Engineering, Dresden University of Technology, Germany
[2] Fraunhofer-Institut für Werkzeugmaschinen und Umformtechnik IWU, Fraunhofer Gesellschaft, Germany
[*] E-mail: yutao.lan@tu-dresden.de
https://doi.org/10.36897/jme/205772

input parameter. Typically, during the design phase, these loads are estimated by means of simulations [6]. However, actual load conditions might differ significantly from simulated values. For effective prediction of an LGW's remaining service life, real-time load measurements are inevitable in terms of understanding the load condition on the system and detecting deviations caused by wear or damage.

Load measurement is primarily based on determining deformation in load-bearing components and converting it into electrical signals [7]. Commonly used sensor types include piezoelectric sensors [8] and strain gauges [9]. They make use of the piezoelectric and the piezoresistive effect, respectively. The conventional measurement method involves installing external force sensors in series with the measuring object. However, due to the compact and integrated nature of LGW systems, attaching external sensors is impractical. Moreover, this method can alter the system's stiffness. To address these challenges, recent research has focused on integrating sensors directly into LGWs. For instance, piezoresistive strain gauges have been embedded in the carriage to measure strain at the contact region of the REs [10, 11] or along the carriage flank [12]. While preliminary results are promising, these approaches require significant modifications to the LGW, which may affect its structural stiffness. Additionally, they involve supplementary electronics and complex signal processing algorithms.

To overcome these limitations, this study proposes a novel load measurement method based on integrated inductive proximity sensors (IPS). Under loading conditions, deformation of the carriage and rolling elements leads to a change in their relative position. The proposed method leverages this distance variation to estimate the load on the LGW system. By analyzing the switching signals of the IPSs, the applied load can be effectively measured without the need for expensive sensors, complex electronics, or sophisticated signal processing algorithms.

This paper is structured as follows: following this introduction, Section 2 presents the methodology of the proposed measurement method. Section 3 describes the experimental setup and procedures in detail. Section 4 discusses the results and highlights the main findings. Finally, Section 5 concludes the study.

2. METHODOLOGY

This section begins with a brief introduction to the selected IPS and the LGW under investigation. Following this, the challenges associated with applying the IPS with respect to the RE are discussed. Key terminology relevant to the measurement approach is then defined and elaborated. Finally, the principle of the proposed novel measurement method is described in detail.

2.1. LINEAR GUIDEWAY

The LGW used in this study is a flanged 25 mm ball rail system with a medium preload of 8%. The carriage and rail are made of carbon steel, manufactured by Bosch Rexroth. The static and dynamic load capacities are 35.9 kN and 28.6 kN, respectively.

2.2. INDUCTIVE PROXIMITY SENSOR

IPSs are commonly used for detecting the presence or absence of metallic objects without physical contact. Their operating principle is based on electromagnetic induction. When a metallic object enters the IPS's electromagnetic field, eddy currents are induced in the object, which in turn disturb the field. Once such a disturbance is detected, a switching signal is triggered [13]. The IPS's characteristics depend on factors such as supply frequency, target distance, material properties and geometry of target [14]. Typically, target geometries used during sensor calibration are circular and of uniform thickness [14]. Consequently, the datasheet specifications (e.g., [15]) generally describe the IPS's behavior only for flat targets. Furthermore, the area of the target is recommended to be at least twice the size of the sensing coil [16]. Since the cross-sectional area of a spherical target varies with distance and can be significantly smaller than the coil area, this introduces additional uncertainty. This uncertainty further emphasizes the need for sensor characterization, which is detailed in Section 3.1.

The IPS was selected for this study due to its simplicity and low cost. Compared to conventional force sensors based on piezoelectric materials, IPS is significantly more affordable. Additionally, the IPS produces a binary output, either "on" or "off", which can be easily processed using a low-cost digital input (DI) circuit, eliminating the need for expensive analog-to-digital converters (ADCs).

The selected IPS model is the E2NC-EDR6-F from Omron, which features a detection range of 0.6 mm and a repeatability of 1 μm.

2.3. SWITCHING BEHAVIOUR OF THE SENSOR WITH RESPECT TO A SPHERICAL OBJECT

As noted in Section 2.2, the IPS's switching behavior with respect to spherical targets is not typically characterized. Since the RE in the LGW is spherical, its interaction with the IPS must be analyzed. This includes evaluating the sensor's detection range, sensitivity, lift-off resolution, and planar resolution, all of which influence the accuracy and reliability of the proposed measurement method (discussed in Section 2.4).

Key definitions are presented below:

Switching distance is defined as the relative distance traveled by a moving RE from the moment it enters the detection range of an IPS to the moment it exits this range. It represents the linear distance over which the object is continuously detected. That is, from the point when the IPS switches to the "on" state to the point when it returns to the "off" state as the object moves through the detection zone. Under constant velocity, the switching distance equals the product of the relative velocity and the time interval during which the IPS remains in the "on" state.

Lift-off resolution is defined as the smallest measurable change in the sensor's vertical distance (lift-off) when aligned with the top of the sphere, as indicated by a change in switching distance. Figure 1 (left) shows a side view of the lift-off between the sensor and the RE. In the Figure 1 (left), the dashed red line represents the sensor's centerline, while the blue line represents the sphere's centerline; both lines are aligned.

Planar resolution is defined as the smallest detectable lateral deviation when the sensor's centerline shifts from alignment with the RE's centerline, as indicated by a change in switching distance. Figure 1 (right) illustrates these definitions.

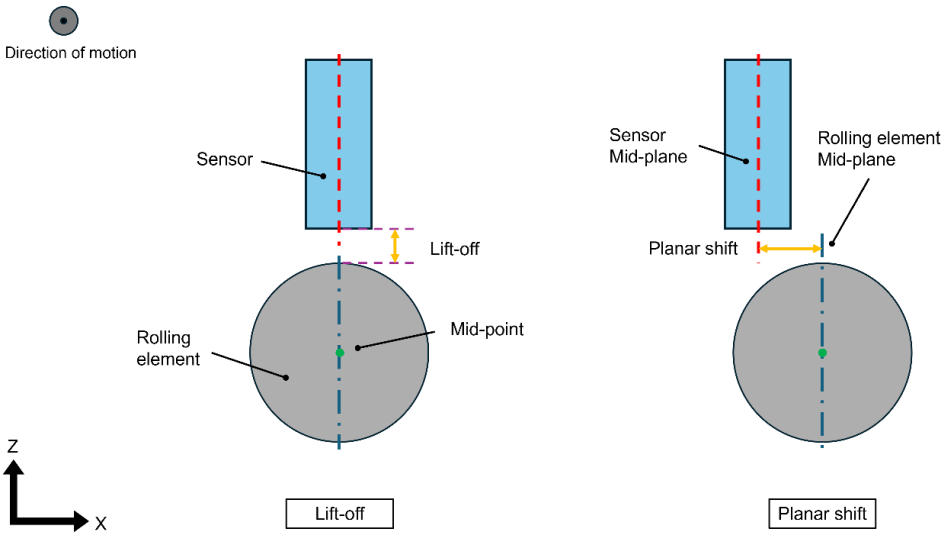

Fig. 1. Relative position between sensor and spherical object: Lift-off (left) and planar shift (right)

2.4. PRINCIPLE OF THE MEASURING METHOD

The proposed method estimates load by detecting changes in the lift-off distance between the RE and the carriage. As the LGW operates, REs periodically pass through the IPS's detection range. The IPS switches on as an RE enters the range and switches off as it exits. The switching distance, the relative displacement between the "on" and "off" signals, depends on the lift-off. At constant relative speed, a shorter lift-off results in a longer switching distance (the IPS stays "on" longer), whereas a greater lift-off shortens this duration.

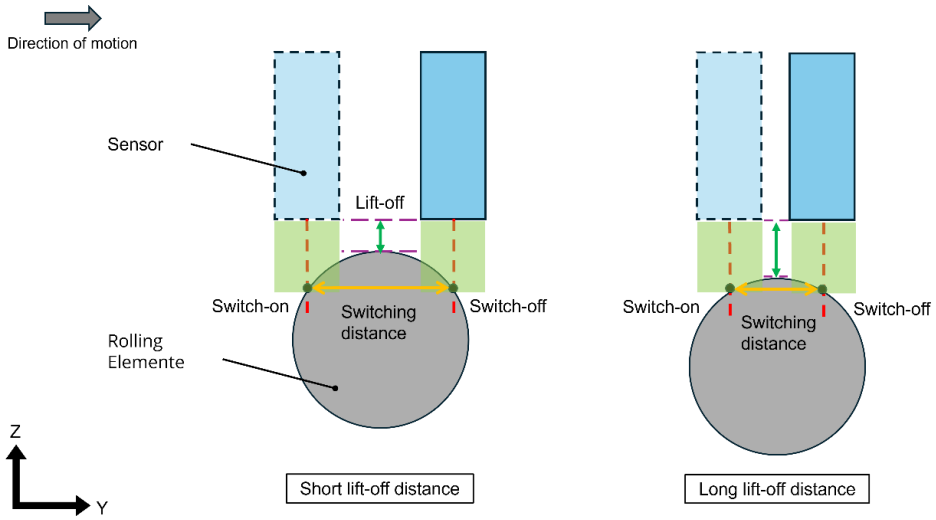

Fig. 2. Principle of the measurement method

Under loading conditions, this lift-off distance varies due to elastic deformation of LWG system. Since the IPS's switching distance depends on the lift-off, it can be used to infer these deformations. This relationship is illustrated in Fig. 2. By continuously monitoring the switching distance, the method enables estimation of lift-off, thereby indirectly measuring deformation in the LGW system under varying load conditions.

3. MATERIAL AND METHOD

This section describes the measurements conducted on two test rigs. The first part focuses on a preliminary investigation carried out on a 3-axis machine tool to characterize the IPS with respect to an RE. The second part details experiments assessing the dependency of switching distance on load.

3.1. CHARACTERIZATION OF THE SENSOR

As discussed in Section 2.2, the behavior of the IPS with respect to a spherical surface is not characterized in standard datasheets. Therefore, a series of experiments were conducted to determine the sensor's detection range, sensitivity, and resolution when interacting with an RE. The experiments were performed using a 3-axis machine tool that provides precise positioning in the x-, y-, and z-coordinates (see Fig. 3), with a repeatability of 0.5 μm. In this experiment, a single RE was placed in a tapered hole on a steel plate. The sensor's lift-off along the z-axis was varied between 0.1 mm and 0.6 mm. The test procedure involved selecting the z-coordinate and keeping it constant for one measurement. Then, the table was moved forwards and backwards (a single cycle) along the y-axis at a specified table velocity from one side of the RE to the other side, as illustrated in the Fig. 3. The position data, table velocity, and switching signals were recorded. This measurement was repeated for a range of x-coordinates, covering the diameter of the RE. Four different velocities were tested: 5 mm/s, 10 mm/s, 25 mm/s, and 100 mm/s. Each configuration was measured three times to ensure repeatability and reduce variability. Simply put, the switching behavior was investigated in terms of the x, y, z-coordinates at 4 different velocities.

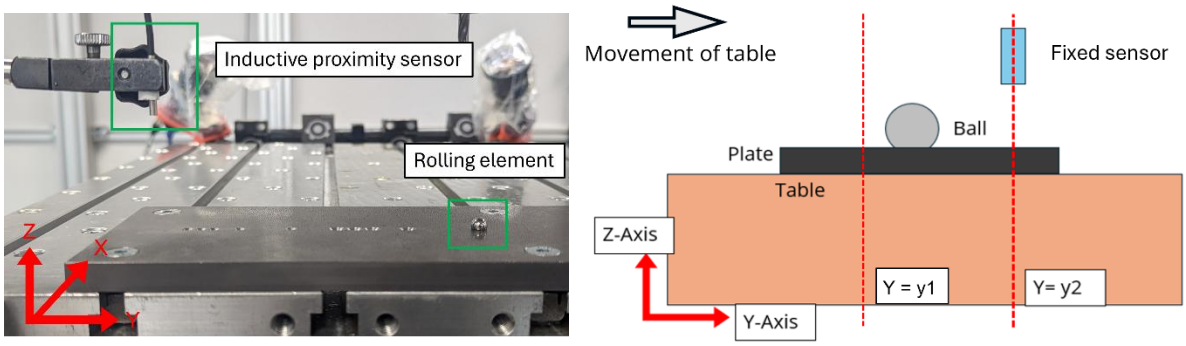

Fig. 3. Test setup on three-axis machine tool

3.2. VALIDATION OF THE MEASUREMENT PRINCIPLE

The experimental setup used in this study was specifically designed to investigate the fatigue life of LGWs. The system features a stationary LGW carriage while the machine's table can be driven linearly along its axis with adjustable velocity and acceleration. Vertical loading was applied using compressible spring columns, with a single column used for this experiment, as shown in Fig. 4.

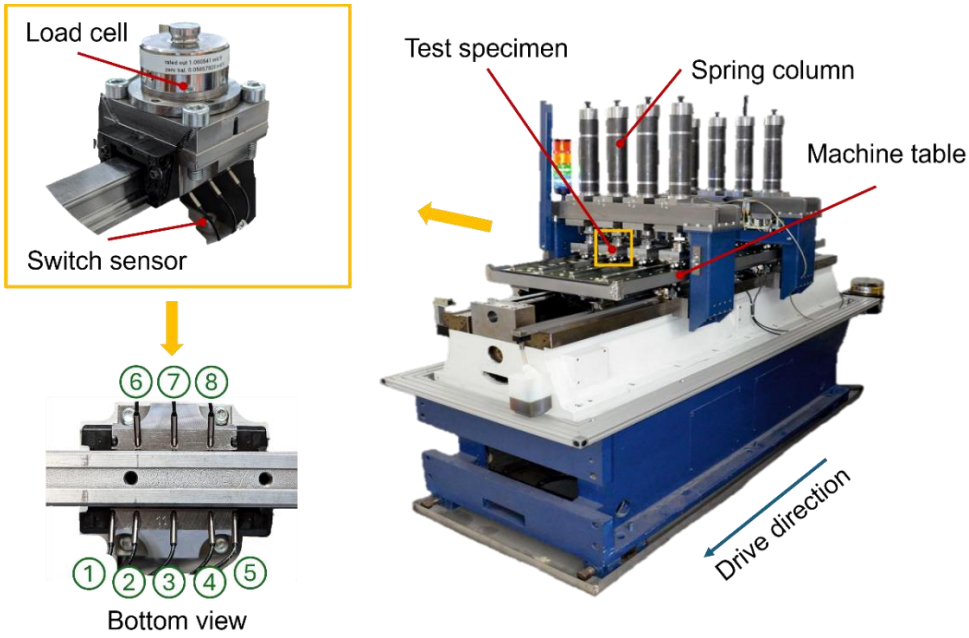

Fig. 4. Test setup and linear guideway fatigue test rig

To ensure that the carriage remained fixed during table movement, it was secured on both sides with an adapter and positioned directly beneath the selected spring column. Precision cut-outs were machined into the LGW carriage to integrate the sensors without additional mounting components. The positions of these cut-outs were placed deliberately with respect to the simulation results of an LGW in [17]. The simulated stress distribution plot of the LWG indicates that the sensors were positioned at places without mechanical stress under compressive loading. By doing so, the cut-outs will not affect the LGW system's stiffness. Adhesive and wax were used to secure the installation. A total of eight sensors were installed in the load zone, three on each side in the middle and two at the edges, as shown in Fig. 4. To measure the applied load, a load cell was positioned directly beneath the load application point of the spring column, as shown in Fig. 4. During testing, the table moved along a 500 mm path under varying loads while data on position, switching distances, and applied forces were collected. Each test consisted of three forward and three return travels. The experiment analyzed the effect of external loads ranging from 90 N to 15,000 N on the sensor's switching distance while the table moved at a constant velocity of 20 mm/s. Note that the table's velocity is twice that of the RE's.

4. RESULTS AND DISCUSSIONS

This section presents and analyzes the results of the experimental research on the characteristics of the IPSs with respect to REs, and the relationship between the sensor's switching distance and the applied load. The research was conducted using a 3-axis machine tool and a fatigue life test rig under vertical compressive load conditions.

4.1. DETECTION RANGE AND SENSITIVITY

The sensor's detection range and sensitivity with respect to REs were evaluated by moving the table of the three-axis machine tool back and forth along the y-axis at a specified lift-off distance. After each cycle, the lift-off distance was incremented in defined steps. This measurement was repeated for various x-coordinates, covering the full width of the RE (see Section 3.1 for details). The switching distance was recorded as a function of lift-off at different table velocities.

The results show that the switching distance in terms of lift-off remained relatively stable regardless of the table velocity, as illustrated in Fig. 5. However, at the highest velocity tested, a slight reduction in switching distance was observed. This deviation is attributed to the sensor's specified response time of 1 ms. Moreover, Fig. 5 indicates a reduced effective detection range of approximately 0.4 mm, compared to the 0.6 mm specified in the manufacturer's datasheet. It was also observed that the sensor's sensitivity is slightly non-linear, with the non-linearity becoming more pronounced at larger lift-off distances.

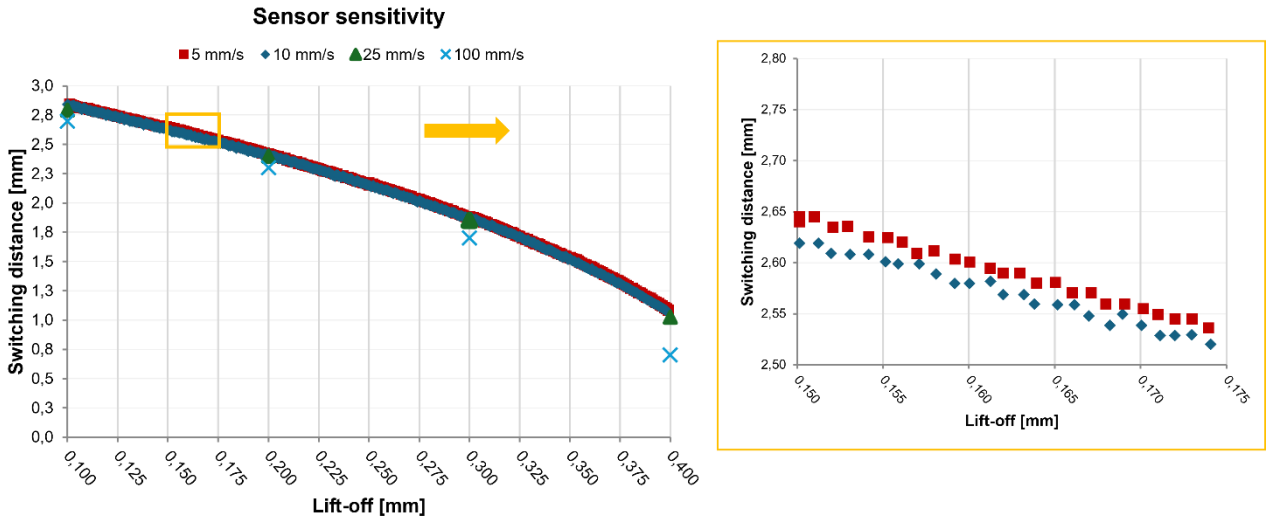

Fig. 5. Sensor detection range and sensitivity

This behavior aligns with the conceptual basis of the measurement method, where the switching distance changes non-linearly due to the curvature of the RE surface (see Fig. 2).

To quantify this non-linearity, linear regression was performed for the tested table velocity of 10 mm/s, and the results are summarized in Table 1.

Table 1. Residual R^2 values of linear regression for different lift-off ranges, at a constant table velocity of 10 mm/s.

Lift-off [mm]	0.1 - 0.2	0.2 - 0.3	0.3 - 0.4	0.1 – 0.4
Residual R^2	0.9987	0.9984	0.9952	0.9841

In an LGW system, the dependency of the deformation on applied load is inherently non-linear, as demonstrated in Fig. 7b and discussed in Section 4.4. In order to distinguish the intrinsic nonlinearity of the LGW system, the non-linearity of the measuring method must be eliminated or mathematically corrected during signal processing. For simplicity, this is achieved in this study by positioning the sensor closer to the object, since the sensitivity is approximately linear in the 0.1 to 0.2 mm lift-off range.

4.2. LIFT-OFF RESOLUTION, PLANAR RESOLUTION AND PLANAR DEAD ZONE

The lift-off resolution of a sensor is defined as the smallest detectable change in vertical distance between the sensor and the RE, as discussed in Section 2.3. To determine this resolution, the same dataset evaluated in Section 4.1 was used. A histogram of the recorded switching distances was generated to determine the maximum number of repetitions of a given switching distance. If each lift-off step corresponds to a unique switching distance, the sensor is considered capable of resolving that step. Otherwise, the number of repetitions indicates the resolution limit. A step size of 1 μm was chosen based on the 0.5 μm repeatability of the 3-axis machine tool. Due to the extensive amount of data, the entire range was covered by three measurement sets. Each set consisted of a lift-off range of 0.1 mm. In the lift-off range between 0.1 and 0.2 mm, the maximum number of repetitions of the same switching distance recorded was 4, corresponding to a lift-off resolution of 4 μm (repetition number times step size). Furthermore, it was observed that the lift-off resolution improves slightly with increasing lift-off distance. This observed tendency is probably attributed to the spherical surface, as the switching distance changes more rapidly with increasing lift-off distance. The resolution values for all ranges tested are summarized in Table 2.

Table 2. Lift-off resolution

Lift-off range [mm]	0.1 to 0.2	0.2 to 0.3	0.3 to 0.4
Resolution [μm]	4	3	2

Planar resolution is defined as the smallest detectable change between the centerlines of the sensor and the RE, as discussed in Section 2.3. To evaluate this parameter, a test step of 10 μm along the x-axis was chosen. Figure 6 shows a representative plot for the result of one measurement. The planar resolution was determined by analyzing a histogram of the switching distance data, taking into account only half of the repetitions due to the symmetry

of the spherical object. It was observed that the switching distance remained unchanged in the vicinity of the RE's mid-plane. In this region, sudden variations in the recorded switching distance were noted, likely corresponding to the RE mid-plane, but these changes did not consistently occur at the exact center. Thus, these data points were excluded from the analysis. This result indicates that the sensor is unable to detect a planar shift near the RE mid-plane, an area that is therefore regarded as the sensor's planar dead zone. The measured planar resolution and planar dead zone values are 50 μm and 260 μm, respectively. The measured values for the planar resolution and dead zone are summarized in Table 3. Overall, these results indicate that the sensor exhibits lower resolution to planar shifts compared to lift-off changes.

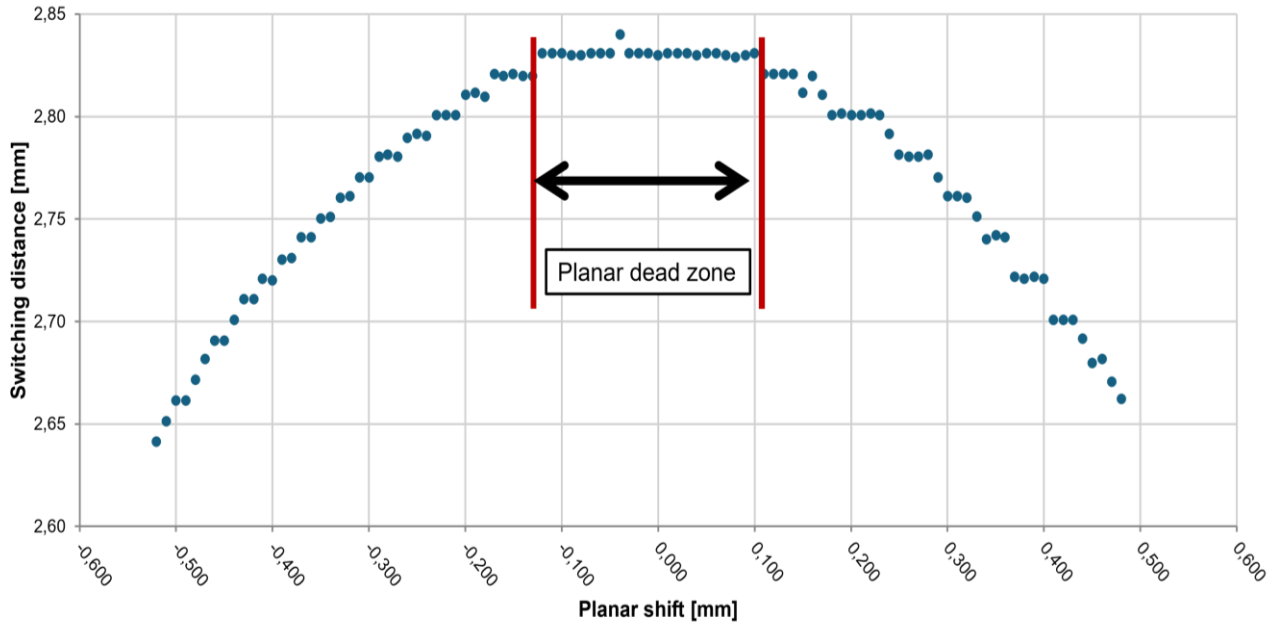

Fig. 6. Dependency of switching distance on planar shift at lift-off 0.1 mm, at a constant table velocity of 10 mm/s

Table 3. Planar resolution and planar dead zone

Lift-Off [mm]	0.1	0.2	0.3	0.4
Planar resolution [μm]	50	50	40	30
Planar dead zone [μm]	220	260	220	170

4.3. SENSOR RESOLUTION IN REAL-WORLD CONTEXT

In practical applications, the sensor is typically pointed to the mid-point of the RE, shown in Fig. 1. The measured planar dead zones are on the order of hundreds of micrometres, whereas the manufacturer's tolerances and potential deformations, such as RE compression under vertical load or carriage flank expansion, are generally limited to tens of microns, as shown in Figure 7b [18]. As a result, the sensor is unlikely to detect any significant planar shifts, implying that it primarily responds to changes in lift-off in real-world settings.

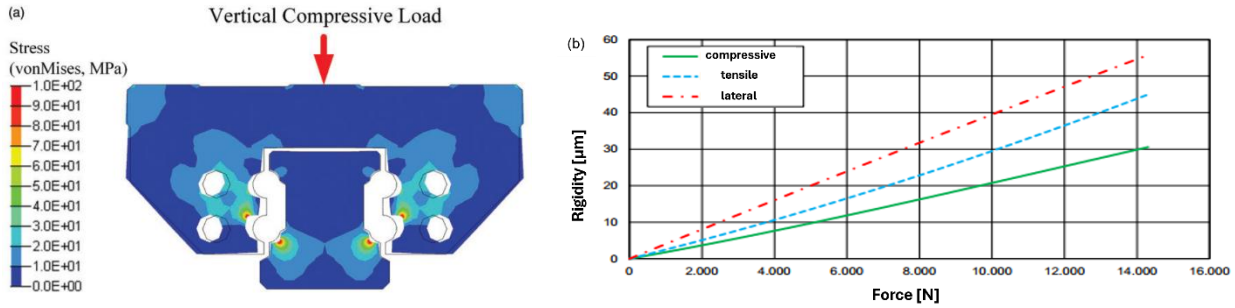

Fig. 7. (a) Elastic deformations and stress contour of the carriage and the rail under vertical compressive load [17]; (b) Deformation under load of the tested linear guideway model KWD25FNS, provided by the Bosch Rexroth [18]

4.4. DEPENDENCY OF THE SENSOR'S SWITCHING DISTANCE ON THE APPLIED LOAD

This section presents the experimental results obtained to evaluate the dependency of the sensor's switching distance on the applied load. In these experiments, the sensors were integrated into the carriage as described in Section 3.2. Figure 8 shows the relationship between the external load applied to the LGW and the sensor's switching distance over a travel range from 0 to 500 mm. For clarity, the 90 N and 1 kN curves are not shown, as they closely overlap with the 2 kN curve. The results confirm the proposed measurement principle: the sensor's switching distance varies with the applied load. Specifically, as the applied force increases, the switching distance decreases. This inverse relationship suggests that increasing load results in a greater distance between the RE and the IPS. This increased distance may be attributed to deformation of the RE or changes in the contact angle between the RE and the rail under higher loading, both of which alter the relative position between the RE and the IPS. However, further investigation is needed to determine the root cause of this relative position change.

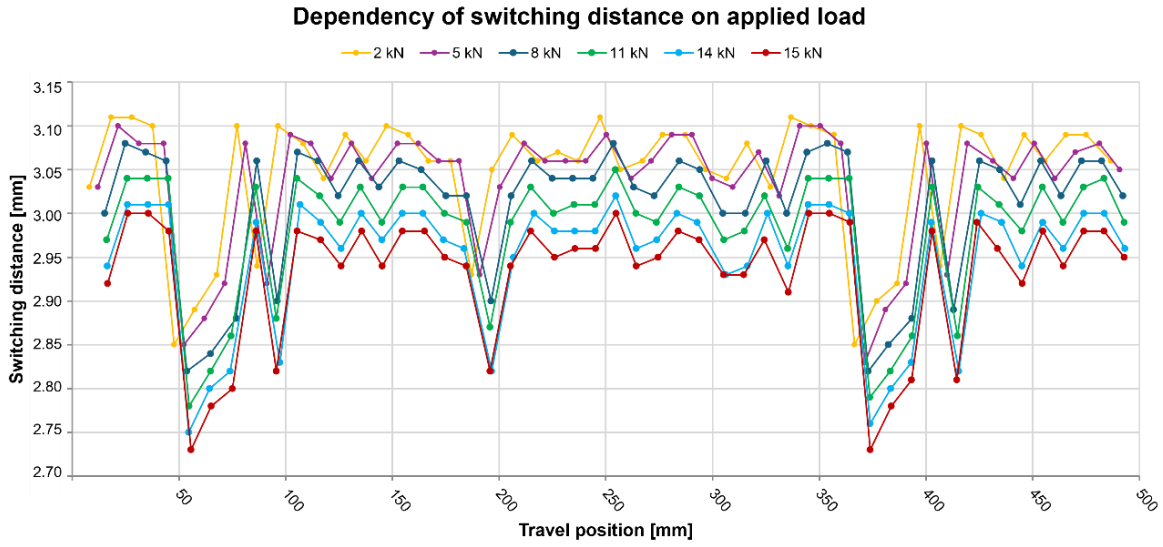

Fig. 8. Dependency of switching distance on load at a constant table velocity of 20 mm/s, sensor 3

To further analyze this dependency, the absolute average change in switching distance and the corresponding load are plotted in Fig. 9. Note that the average change in switching distance is negative, meaning that the lift-off distance is increasing. The data show that three sensors mounted on the same side of the carriage exhibit similar trends. The discrepancy between the sensors might arise due to their lift-off distance, as the linearity of the sensor's sensitivity changes with different lift-off distances, as shown in Figure 5. It is observed that the relationship between the applied force and the sensor's switching distance is slightly non-linear. Notably, the slope of the curves changes after approximately 5 kN. This inflection point reflects the intrinsic stiffness characteristics of the LWGs. Specifically, when the load exceeds the lift-off force, approximately 6 kN in the tested model, the REs in the upper grooves are no longer engaged, and the load is transmitted solely through the REs in the lower grooves. This reduction in the number of engaged REs results in a corresponding change in stiffness, as can be clearly seen in Fig. 9.

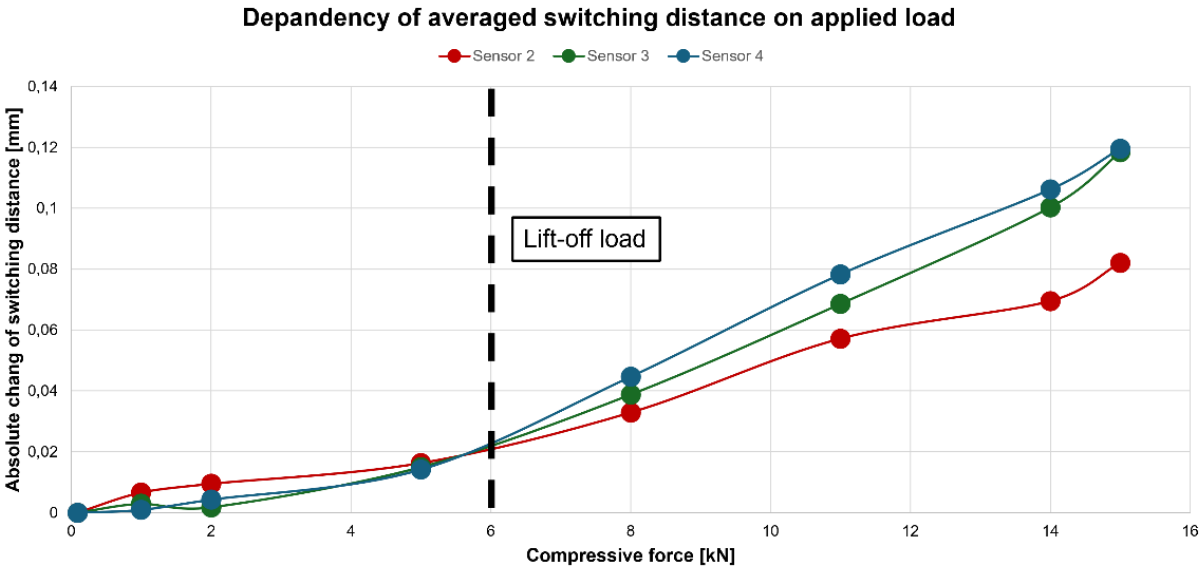

Fig. 9. Dependency of absolute change in averaged switching distance on applied load at a constant table velocity of 20 mm/s

5. CONCLUSION

In this paper, a novel load measurement method for LGWs utilizing integrated IPS has been proposed. The method estimates deformation in the LGW by measuring variations in the vertical distance (lift-off) between the carriage and the RE, based on the IPS's switching signals. Specifically, the lift-off is derived from the switching distance, defined as the relative distance traveled by a moving RE from the moment it enters the detection range of an IPS until it exits this range. The measurement principle was initially validated in a preliminary study using a single IPS and a single RE on a 3-axis machine tool. The results demonstrated that the IPS could measure lift-off changes within a 0.4 mm range, with a precision of 4 μm.

The method was further evaluated on a fatigue life test rig equipped with an IPS-integrated carriage under various load conditions. This second study revealed a strong correlation between the switching distance and the applied load, with a maximum switching distance change of 0.12 mm recorded under a load of 15 kN. Overall, the results confirm the feasibility and effectiveness of the proposed method for real-time load monitoring in linear guideway systems, offering a low-cost and compact alternative to conventional force measurement methods.

ACKNOWLEDGEMENTS

This project has received funding from the German Research Foundation (DFG) under grant agreement No. 499035309.

REFERENCES

[1] MOURTZIS D., 2021, *Towards the 5th Industrial Revolution: A Literature Review and a Framework for Process Optimization Based on Big Data Analytics and Semantics*, Journal of Machine Engineering, 21/3, 5–39, https://doi.org/10.36897/jme/141834.

[2] OHTA H., TANAKA K., 2009, *Vertical Stiffnesses of Preloaded Linear Guideway Type Ball Bearings Incorporating the Flexibility of the Carriage and Rail*, Journal of Tribology 132 /1, https://doi.org/10.1115/1.4000277.

[3] IHLENFELDT S., MÜLLER J., STAROSZYK D., 2020, *Lifespan Investigations of Linear Profiled Rail Guides at Pitch and Yaw Moments, Production at the Leading Edge of Technology*, Springer Berlin Heidelberg, 294–303, https://doi.org/10.1007/978-3-662-62138-7_30.

[4] TAO W., ZHONG Y., FENG H., WANG Y., 2013, *Model for Wear Prediction of Roller Linear Guides*, Wear 305 (1-2) 260-266, https://doi.org/10.1016/j.wear.2013.01.047.

[5] STAROSZYK D., MÜLLER J., IHLENFELDT S., 2024, *Increasing the Service Life Prediction Accuracy of Linear Guideways Considering Real Operating Conditions*, Mechanism and Machine Theory 201, 105734, https://doi.org/10.1016/j.mechmachtheory.2024.105734.

[6] STAROSZYK D., MÜLLER J., IHLENFELDT S., 2024, *Simplification of the Rolling Contact-Related Lifetime Calculation of Profiled Rail Guides with a Polynomial Regression*, Journal of Machine Engineering 24/1, 60–73, https://doi.org/10.36897/jme/186130.

[7] Morris A. and Langari R., 2012. *Measurement and Instrumentation – Theory and Application*, Elsevier, https://doi.org/10.1016/C2009-0-63052-X

[8] SIMS N.D., BAYLY P.V., YOUNG K.A., 2005, *Piezoelectric Sensors and Actuators for Milling Tool Stability Lobes*, Journal of Sound and Vibration 281 (3-5), 743–762, https://doi.org/10.1016/j.jsv.2004.02.014.

[9] KEIL S., 2017, *Technology and Practical Use of Strain Gages with Particular Consideration of Stress Analysis Using Strain Gages: with Particular Consideration of Stress Analysis Using Strain Gages*, Wilhelm Ernst & Sohn, https://doi.org/10.1002/9783433606667.

[10] KRAMPERT D., UNSLEBER S., REINDL L., 2020, *Measuring Load on Linear Guides in Different Load Scenarios Using an Integrated DLC Based Sensor System*, in: SMSI 2020 – Sensors and Instrumentation, https://doi.org/10.5162/SMSI2020/A4.4.

[11] KRAMPERT D., UNSLEBER S., JANSSEN C., REINDL L., 2019, *Load Measurement in Linear Guides for Machine Tools*, Sensors, 19/15, 3411, https://doi.org/10.3390/s19153411.

[12] KRAMPERT D., UNSLEBER S., REINDL L., 2021, *Localized Surface Strain Measurement for Load Detection Using Diamond Like Carbon Coating on a Linear Guide*, 2021 IEEE International Instrumentation and Measurement Technology Conference (I2MTC), IEEE, https://doi.org/10.1109/i2mtc50364.2021.9459827.

[13] TUMANSKI S., 2007, *Induction Coil Sensors-a Review*, Measurement Science and Technology, 18/3, IOP Publishing p. R31-R46, https://doi.org/10.1088/0957-0233/18/3/r01.

[14] BARTOLETTI C., BUONANNI R., FANTASIA L.G., FRULLA R., GAGGIOLI W., SACERDOTI G., 1998, *The Design of a Proximity Inductive Sensor*, Measurement Science and Technology, 9/8, IOP Publishing 1180–1190, https://doi.org/10.1088/0957-0233/9/8/007.

[15] Omron, Smart Proximity Sensor – E2NC Series Data Sheet, https://www.ia.omron.com/products/family/3700/download/catalog.html, accessed: 2025-04-12.

[16] Texas Instruments, 2021, *Sensor Design for Inductive Sensing Applications Using LDC*, chrome-extension://efaidnbmnnnibpcajpcglclefindmkaj/https://www.ti.com/lit/an/snoa930c/snoa930c.pdf?ts=1744988248220, accessed: 2025-04-18.

[17] YANG L., WANG L., ZHAO W., 2020, *Hybrid Modeling and Analysis of Multidirectional Variable Stiffness of the Linear Rolling Guideway Under Combined Loads*, Proceedings of the Institution of Mechanical Engineers, Part C: Journal of Mechanical Engineering Science 234 /13, 2716-2727, https://doi.org/10.1177/0954406220908894.

[18] BOSCH REXOROTH, *Linear Motion Technology Handbook*, https://www.boschrexroth.com/en/us/media-details/c3554fde-8a09-471e-b6bf-c52a8bbf54e0, accessed: 2025-01-29.